User and Content Dynamics of Edge-Aided Immersive Reality Services

Olga Chukhno, *Graduate Student Member, IEEE*, Olga Galinina, *Member, IEEE*, Sergey Andreev, *Senior Member, IEEE*, Antonella Molinaro, and Antonio Iera, *Senior Member, IEEE*

***Abstract*—This letter presents a practice-inspired methodology for characterizing the user and content dynamics of extended reality (XR) services over wireless networks. The proposed approach is based on a fluid approximation to capture the time and space dynamics of XR content exchange during its transient phase while considering both radio communication and edge computing resources. Hence, our methodology provides an effective tool to support resource assignment for radio and computing in 5G and beyond networks, especially under non-stationary processes with time-varying traffic arrivals, such as those with a periodic arrival rate function.**

***Index Terms*—5G+ connectivity, wireless communications, edge computing, immersive reality, user and content dynamics.**

I. Introduction

With the increasing consumer interest in immersive applications, extended reality (XR) technology is rapidly advancing toward its mass adoption. Compared to traditional technologies, XR services offer higher user mobility and interaction freedom. The incorporation of wireless network solutions in XR services, e.g., [1], has further facilitated user motion and introduced new challenges, such as user/content dynamics and performance evolution, thereby requiring careful consideration and innovative solutions.

In the literature, XR systems are usually assessed in steady-state operating conditions [2], [3]. However, due to the recent developments in the context of XR interaction, state-of-the-art modeling solutions may have limited applicability to practical XR deployments. A major challenge is to accurately model the *dynamic* and *non-stationary* [4] aspects inherent to the operating behavior of modern immersive reality systems in the presence of periodic arrival processes [5]. Addressing that is crucial to provide network engineers with an effective means to plan and optimize radio and computing resources by taking into account the specific features of XR.

To capture the time and space dynamics and the system effects in a transient phase of XR operation, the actual discrete numbers of users engaged in XR content exchange can be approximated with an equivalent continuous process. For example, in [6], a fluid approximation is used to model the evolution of vehicles along a highway. Further, in [7] and [8], the numbers of users retrieving the content and those who have already received it are represented as continuous flows. In wireless sensor networks, the volume of traffic is also modeled using macroscopic fluid dynamic models [9].

By their design, XR systems have a unique set of features, including form factor constraints, which impose strict requirements on power consumption and heat dissipation of user equipment. Therefore, content processing may not always be conducted on the XR head-mounted displays (HMDs), thus requiring task offloading to an edge server over a wireless network. As a result, analyzing XR content exchange dynamics requires the consideration of both *radio communication* and *edge computing* resources. This letter addresses the challenge of modeling the *dynamics* and *non-stationarity* of emerging XR systems by bridging the gap between traditional steady-state assessments and practical XR technology deployments.

We thereby offer a practice-inspired methodology to characterize the evolution of users utilizing XR services in radio networks as a continuous fluid, thus providing insights into XR content dynamics. Specifically, we model the dynamic behavior of XR services with periodic arrivals and consider the departure rate that is determined by the communication and computing characteristics of the 5G New Radio (NR) and edge technologies. We then apply our fluid approximation-based methodology to assess the XR system performance under characteristic deployment setups.

II. System Model

We consider an outdoor environment where multiple homogeneous users engage in an interactive XR experience through HMDs. As XR devices have limited computing performance due to constraints on their size, power consumption, and heat dissipation, we assume that an HMD acts as a thin client by receiving personalized video streams from a proximate edge computing server. The server is co-located with a 5G base station (BS), as illustrated in Fig. 1, and connects to HMDs over a wireless link using, for example, millimeter-wave radio technology.

Assumption 1 (User State): The XR services involve users sending location and motion information to the BS, which is then used to process the corresponding video on an edge server. Hence, a user can be in one of the three states: (i) an *active communicating user* sending the location and

Manuscript received 11 March 2023; revised 10 May 2023; accepted 04 June 2023. Date of publication 15 June 2023; date of current version 2 January 2024. This work was supported in part by the European Union's Horizon 2020 Research and Innovation Programme under the Marie Skłodowska-Curie under Grant 813278 (A-WEAR; http://www.a-wear.eu/) and in part by the Academy of Finland through Project RADIANT, Project IDEA-MILL, and Project SOLID. The associate editor coordinating the review of this article and approving it for publication was E. E. Tsiropoulou. *(Corresponding author: Olga Chukhno.)*

Olga Chukhno is with the DIIES Department, University Mediterranea of Reggio Calabria, 89124 Reggio Calabria, Italy, also with CNIT, 56127 Pisa, Italy, and also with the Unit of Electrical Engineering, Tampere University, 33014 Tampere, Finland (e-mail: olga.chukhno@unirc.it).

Olga Galinina is with the Unit of Electrical Engineering, Tampere University, 33014 Tampere, Finland, and also with the Tampere Institute for Advanced Study, 33014 Tampere, Finland (e-mail: olga.galinina@tuni.fi).

Sergey Andreev is with the Unit of Electrical Engineering, Tampere University, 33014 Tampere, Finland (e-mail: sergey.andreev@tuni.fi).

Antonella Molinaro is with the DIIES Department, University Mediterranea of Reggio Calabria, 89124 Reggio Calabria, Italy, and also with CNIT, 56127 Pisa, Italy (e-mail: antonella.molinaro@unirc.it).

Antonio Iera is with the DIMES Department, University of Calabria, 87036 Arcavacata, Italy, and also with CNIT, 56127 Pisa, Italy (e-mail: antonio.iera@dimes.unical.it).

Digital Object Identifier 10.1109/LNET.2023.3286581

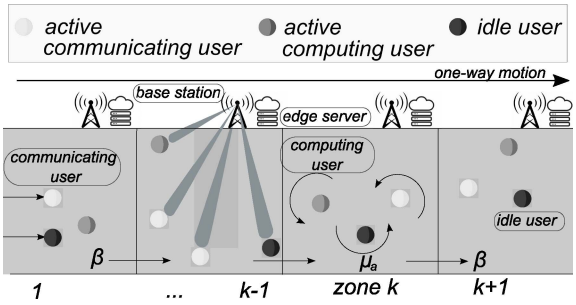

Fig. 1. Dynamic XR system illustration.

motion information to the server, (ii) an *active computing user* processing XR 360° video on the server, or (iii) an *idle user*.

Active users transition to the idle state only after completing their uplink transmission and processing the required content at the edge, i.e., after passing through both communication (transmission) and processing (computing) states. In turn, idle users switch to the active communicating state based on their content demand, thus resulting in a transition rate μ_a, which corresponds to the average value commonly employed to model systems with homogeneous user behavior. While we assume that μ_a does not vary over time, our methodology can also incorporate time-varying dependencies if needed.

Assumption 2 (User Motion): We consider one-way motion around a semi-infinite pedestrian area. For example, users may traverse from one XR-ready area to another or follow a straight path along the street. We note that such one-way motion can readily be generalized to a two-way traffic scenario. The pedestrian area is divided into K zones, each served by a 5G BS. Both active and idle users move within pedestrian zone $k \in \mathcal{K} = \{1, \ldots, K\}$ with an average velocity v.

Assumption 3 (System Dynamics): We consider the following arrivals of active and idle users into the system:

1) zone 1: external *active communicating* or *idle* users;
2) zone k: *active communicating* or *active computing* or *idle* users from zone $k-1$ arriving with rate β;
3) zone k: transition from *idle* to *active communication* due to an initiated transmission with rate μ_a;
4) zone k: transition from *active communication* to *active computing* due to a completed transmission;
5) zone k: transition from *active computing* to *idle* due to a completed content processing at the edge node.

As an example, we assume a periodic external arrival rate typical for XR services [5], which varies between the minimum and the maximum values as a sine function. To control arrivals in time, we additionally parameterize such processes using phase shifts w_0^a and w_0^d and angular frequencies w^a and w^d for active and idle users, correspondingly. Angular frequency is thus related to the period T as $w = 2\pi T$. We limit the maximum and minimum values of the external arrival rate by λ_1^a, λ_1^d and λ_2^a, λ_2^d, respectively. Therefore, the external arrival rate for actively communicating and idle users at time t may be expressed as

$$\lambda^a(t) = \sin(w^a t + w_o^a)(\lambda_1^a - \lambda_2^a)/2 + (\lambda_1^a + \lambda_2^a)/2, \quad (1)$$

$$\lambda^d(t) = \sin(w^d t + w_o^d)(\lambda_1^d - \lambda_2^d)/2 + (\lambda_1^d + \lambda_2^d)/2. \quad (2)$$

Assumption 4 (Communication (Transmission) State): Each 5G BS serving a given zone k provides wireless connectivity to the users within it. We require that the available radio resources at each BS are sufficient and are equally shared in time and frequency among $N_k^{at}(t)$ active users during the transmission phase at time t.

Further, we assume that B_t is the average uplink packet size and R_0^t is the total uplink capacity (in bits per second). In the case of $N_k^{at}(t)$ participants, we may express the transition rate of users from their status of *active in the communication phase* (i.e., transmitting) to that of *active in the processing phase* (i.e., their content is being processed) as

$$C^t(t) = \frac{1}{N_k^{at}(t)} \cdot C_0^t, \text{ where } C_0^t = R_0^t / B_t. \quad (3)$$

Assumption 5 (Processing (Computing) State): The BS that serves zone k is associated with an edge node, wherein multiple virtual machines (VMs) are utilized to implement parallel processing of content. To take into account the input/output interference among VMs of the same node, we introduce a degradation factor d [10], so that the individual share of the available resources in the case of $N_k^{ac}(t)$ active computing users in zone k is estimated as $[N_k^{ac}(t)(1+d)^{(N_k^{ac}(t)-1)}]^{-1}$ [11].

If B_c is the average size of the uploaded content (in bits), C_c is the computational intensity (in CPU cycles per bit) required to process the content, and R_0^c is the processing capacity (in CPU cycles per second) of the edge node, then the actual transition rate from the user status of *active in the processing phase* (i.e., content is being processed) to that of *idle* (i.e., content processing completed) can be determined as

$$C^c(t) = \frac{1}{N_k^{ac}(t)(1+d)^{(N_k^{ac}(t)-1)}} \cdot C_0^c, \text{ where } C_0^c = \frac{R_0^c}{B_c C_c} \quad (4)$$

and $1/C_0^c$ represents the time for processing the received content at the edge node. For the sake of analytical tractability, we modify the shape of (4) as

$$C^c(t) = \frac{1}{N_k^{ac}(t)(N_k^{ac}(t)+\alpha)} \cdot C_0^c, \quad (5)$$

where α is a fitting parameter obtained numerically to approximate (4).

We note that specific distributions of file size, channel conditions, and data/computing rates can be readily incorporated into the considered average parameters. As a result, our system model offers a general but accurate representation of XR user and content dynamics, which is validated in Section IV below.

III. Fluid Approximation

In this section, we detail the proposed methodology to evaluate the performance of a dynamic XR system. We employ a fluid approximation, which allows replacing integer-valued processes with deterministic real-valued alternatives and is particularly well-suited for analyzing non-stationary systems.

We denote the total numbers of idle and active users in the communication and processing states within zone k at time t as $N_k^d(t)$, $N_k^{at}(t)$, and $N_k^{ac}(t)$, respectively, and consider them as non-negative real numbers. Further, let $C_k^{a_t+}(t)/C_k^{a_t-}(t)$ and $C_k^{a_c+}(t)/C_k^{a_c-}(t)$ be the numbers of active communicating and computing users that arrive in/depart from zone k during the time interval $(0, t]$. Similarly, $C_k^{d+}(t)/C_k^{d-}(t)$ represent the respective numbers of idle users arriving in/departing from zone k during time (0, t]. For the sake of clarity, we further omit index (t).

TABLE I
EXPRESSIONS FOR ARRIVING/DEPARTING FLOWS IN (9)

$C_1^{a_t+} = \lambda^a + \mu_a N_1^d$	$C_1^{a_t-} = C_0^t + \beta N_1^{at}$
$C_1^{a_c+} = C_0^t$	$C_1^{a_c-} = \frac{C_0^c}{(N_1^{ac}+\alpha)} + \beta N_1^{ac}$
$C_1^{d+} = \lambda^d + \frac{C_0^c}{(N_1^{ac}+\alpha)}$	$C_1^{d-} = \mu_a N_1^d + \beta N_1^d$
$C_k^{a_t+} = \mu_a N_k^d + \beta N_{k-1}^{at}$	$C_k^{a_t-} = C_0^t + \beta N_k^{at}$
$C_k^{a_c+} = C_0^t + \beta N_{k-1}^{ac}$	$C_k^{a_c-} = \frac{C_0^c}{(N_k^{ac}+\alpha)} - \beta N_k^{ac}$
$C_k^{d+} = \frac{C_0^c}{(N_k^{ac}+\alpha)} + \beta N_{k-1}^d$	$C_k^{d-} = \mu_a N_k^d + \beta N_1^d$
$\lambda^a = \sin(w^a t + w_o^a)\frac{\lambda_1^a - \lambda_2^a}{2} + \frac{\lambda_1^a + \lambda_2^a}{2}$	
$\lambda^d = \sin(w^d t + w_o^d)\frac{\lambda_1^d - \lambda_2^d}{2} + \frac{\lambda_1^d + \lambda_2^d}{2}$	

The evolution of the numbers of active and idle users in zone k is governed by a system of ordinary differential equations (ODEs) for $x_k \geq 0$, $0 < t < \infty$, $k \in \mathcal{K}$, as

$$\begin{cases} \frac{dN_k^{at}}{dt} \equiv C_k^{a_t+} - C_k^{a_t-}, \\ \frac{dN_k^{ac}}{dt} \equiv C_k^{a_c+} - C_k^{a_c-}, \\ \frac{dN_k^{d}}{dt} \equiv C_k^{d+} - C_k^{d-}, \end{cases} \tag{9}$$

where variables $C_k^{d/a+/-}$ are collected in Table I.

We assume that the content requests start at $t = 0$, where the number of idle users in zone k equals M_k, which defines the initial conditions for (9). Expanding (9), we arrive at the Cauchy problem in (6), which determines the numbers of active users during the communication and computing phases and idle users, N_k^{at}, N_k^{ac}, and N_k^d.

We solve the system in (6) by substituting $N_k = N_k^{at} + N_k^{ac} + N_k^d$ and obtain the following:

$$\begin{cases} dN_1/dt = \sin(w^a t + w_o^a)\frac{\lambda_1^a - \lambda_2^a}{2} + \frac{\lambda_1^a + \lambda_2^a}{2} \\ \qquad + \sin(w^d t + w_o^d)\frac{\lambda_1^d - \lambda_2^d}{2} + \frac{\lambda_1^d + \lambda_2^d}{2} - \beta N_1, \\ dN_k/dt = \beta N_{k-1} - \beta N_k. \end{cases} \tag{10}$$

Based on the first ODE in (10), we may obtain the number of users in zone 1 as

$$N_1 = C_1 e^{-\beta t} + H, \tag{11}$$

where constant C_1 is defined by the initial conditions, while H and C_1 are given by expressions (7) and (8), correspondingly.

Further, using (11), we may obtain the total number N_k for $k = i + 4m$, where $i = 1, 2, 3, 4$ and $m \geq 0$, as follows:

$$\begin{cases} N_{k=1+4m} = Z_0 + \beta Z_1^a - w^a Z_2^a + \beta Z_1^d - w^a Z_2^d, \\ N_{k=2+4m} = Z_0 - \beta Z_2^a - w^a Z_1^a - \beta Z_2^d - w^d Z_1^d, \\ N_{k=3+4m} = Z_0 - \beta Z_1^a + w^a Z_2^a - \beta Z_1^d + w^d Z_2^d, \\ N_{k=4+4m} = Z_0 + \beta Z_2^a + w^a Z_1^a + \beta Z_2^d + w^d Z_1^d, \end{cases} \tag{12}$$

where parameters Z_0, $Z_{1/2}^a$, and $Z_{1/2}^d$ are given by

$$\begin{cases} Z_0 = \sum_{n=1}^k \frac{(\beta t)^{k-n} e^{-\beta t}}{(k-n)!} C_n + \frac{\lambda_1^a + \lambda_2^a + \lambda_1^d + \lambda_2^d}{2\beta}, \\ Z_1^a = \frac{(\lambda_1^a - \lambda_2^a)\sin(w^a t + w_0^a)}{2w^{a(k-1)}(\beta^2 + w^{a2})}, Z_2^a = \frac{(\lambda_1^a - \lambda_2^a)\cos(w^a t + w_0^a)}{2w^{a(k-1)}(\beta^2 + w^{a2})}, \\ Z_1^d = \frac{(\lambda_1^d - \lambda_2^d)\sin(w^d t + w_0^d)}{2w^{d(k-1)}(\beta^2 + w^{d2})}, Z_2^d = \frac{(\lambda_1^d - \lambda_2^d)\cos(w^d t + w_0^d)}{2w^{d(k-1)}(\beta^2 + w^{d2})}. \end{cases} \tag{13}$$

Knowing the total number of users, N_k, we may derive N_k^{at}, N_k^{ac}, and N_k^d separately as

$$N_k^{at} = C_{at_k} e^{-\beta t} + H, \tag{14}$$

$$N_k^{ac} = C_{ac_k} e^{-\beta t} + H, \tag{15}$$

$$N_k^d = C_k e^{-\beta t} - C_{at_k} e^{-\beta t} - C_{ac_k} e^{-\beta t} - H, \tag{16}$$

where C_{at_k} and C_{ac_k} can be established for any zone k by substituting (14)-(16) into the initial conditions of (6). This straightforward technical work is left out of scope here.

In summary, this section details the fluid approximation method to characterize the non-stationary evolution process of the numbers of users engaged in XR content exchange under periodic user arrivals. We derive (12) to express the total number of users, while the numbers of idle and active users in the communication and processing states can be obtained with (14)-(16).

IV. NUMERICAL RESULTS

Our simulation setup models a large social/public XR event, e.g., a concert or an outdoor exhibition, where user HMDs offload their extensive computations to the edge. We study the time and space dynamics of users engaged in XR content exchange captured by our deterministic fluid model in Section III and Monte Carlo simulations. The simulation data (see "S" curves) agree with the analytical results (marked as "A") for all of the considered metrics of interest.

$$\begin{cases} dN_1^{at}/dt = (\sin(w^a t + w_o^a)\frac{\lambda_1^a - \lambda_2^a}{2} + \frac{\lambda_1^a + \lambda_2^a}{2}) + \mu_a N_1^d - C_0^t - \beta N_1^{at}, \\ dN_1^{ac}/dt = C_0^t - \frac{C_0^c}{(N_1^{ac}+\alpha)} - \beta N_1^{ac}, \\ dN_1^{d}/dt = (\sin(w^d t + w_o^d)\frac{\lambda_1^d - \lambda_2^d}{2} + \frac{\lambda_1^d + \lambda_2^d}{2}) + \frac{C_0^c}{(N_1^{ac}+\alpha)} - \mu_a N_1^d - \beta N_1^d, \\ dN_k^{at}/dt = \mu_a N_k^d + \beta N_{k-1}^{at} - C_0^t - \beta N_k^{at}, \\ dN_k^{ac}/dt = C_0^t + \beta N_{k-1}^{ac} - \frac{C_0^c}{(N_k^{ac}+\alpha)} - \beta N_k^{ac}, \\ dN_k^{d}/dt = \frac{C_0^c}{(N_k^{ac}+\alpha)} + \beta N_{k-1}^d - \mu_a N_k^d - \beta N_k^d, \\ \text{under initial conditions: } N_1^{at}\big|_{t=0} = 0,\ N_1^{ac}\big|_{t=0} = 0,\ N_1^d\big|_{t=0} = M_1,\ N_k^{at}\big|_{t=0} = 0,\ N_k^{ac}\big|_{t=0} = 0,\ N_k^d\big|_{t=0} = M_k. \end{cases} \tag{6}$$

$$H = \frac{\lambda_1^a + \lambda_2^a + \lambda_1^d + \lambda_2^d}{2\beta} + \frac{(\lambda_1^a - \lambda_2^a)(\beta\sin(w^a t + w_0^a) - w^a\cos(w^a t + w_0^a))}{2(\beta^2 + w^{a2})} + \frac{(\lambda_1^d - \lambda_2^d)(\beta\sin(w^d t + w_0^d) - w^d\cos(w^d t + w_0^d))}{2(\beta^2 + w^{d2})}, \tag{7}$$

$$C_1 = M_1 - \frac{\lambda_1^a + \lambda_2^a + \lambda_1^d + \lambda_2^d}{2\beta} - \frac{(\lambda_1^a - \lambda_2^a)(\beta\sin(w_0^a) - w^a\cos(w_0^a))}{2(\beta^2 + w^{a2})} - \frac{(\lambda_1^d - \lambda_2^d)(\beta\sin(w_0^d) - w^d\cos(w_0^d))}{2(\beta^2 + w^{d2})}. \tag{8}$$

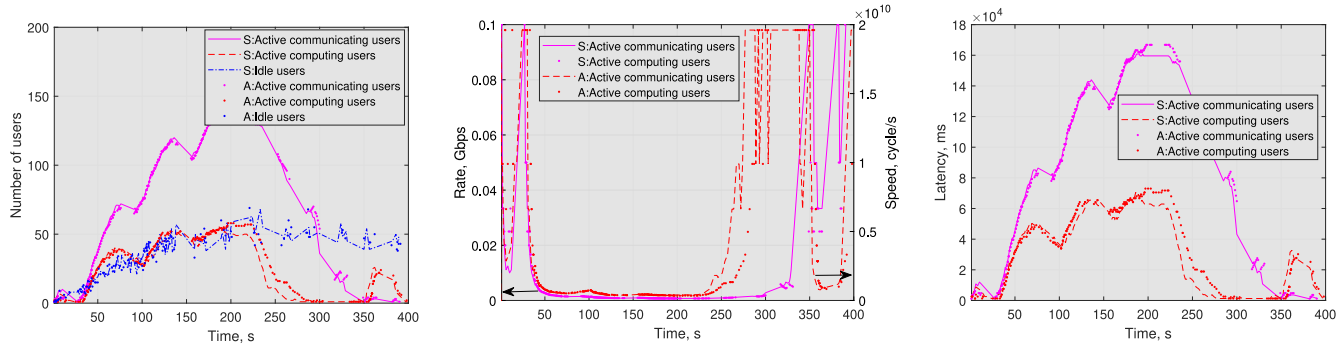

(a) Number of users (b) Actual transmission rate/processing speed (c) Latency

Fig. 2. Performance assessment (Scenario 1): $B_t = 15\,\text{MB}$, $R_0^t = 100\,\text{Mbps}$, $B_c = 30\,\text{MB}$, $R_0^c = 20\,\text{GHz}$.

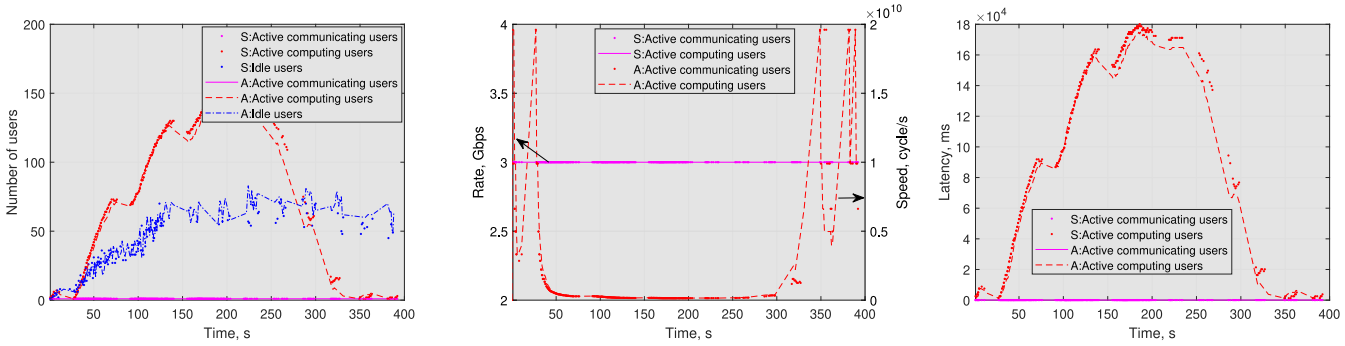

(a) Number of users (b) Actual transmission rate/processing speed (c) Latency

Fig. 3. Performance assessment (Scenario 2): $B_t = 15\,\text{MB}$, $R_0^t = 3000\,\text{Mbps}$, $B_c = 30\,\text{MB}$, $R_0^c = 20\,\text{GHz}$.

TABLE II
MODELING PARAMETERS

Parameter	Values for 3 scenarios
Area	200 m x 50 m [12]
Carrier frequency, f_c	28 GHz [13]
Number of BSs	1 BS per zone [14]
Number of edge servers	1 server per zone [14]
User average velocity	1.55 m/s [15]
Uplink average packet size, B_t	15 MB [16]
Average content size, B_c	30 MB [17]
Computational intensity, C_c	10^3 cycles/bit [18]
Total uplink capacity, R_0^t	100/3000/3000 Mbps [16]
Total processing capacity, R_0^c	20/20/175 GHz [19], [20]
Fitting parameter, α	0.12
Transition rate, μ_a	0.6^{-1} s^{-1}
Phase constants, w_o^a, w_o^d	$\pi, \pi/4$
Angular frequencies, w^a, w^d	$\pi/32, \pi/16$
Maximum values of arrival rate, λ_1^a, λ_1^d	$2, 1$ s^{-1}
Minimum values of arrival rate, λ_2^a, λ_2^d	$0, 0$ s^{-1}

In simulations, the transition rate to the idle state is set as per (4), while when applying our analytical model, we employ the approximation in (5). Our additional results confirm that (5) with $\alpha = 0.12$ closely matches (4). We examine the XR system performance in terms of the number of users, transmission rate[1]/processing speed,[2] and latency. To evaluate the performance of a dynamic XR system, we consider three scenarios with varying levels of radio and computing resources. Scenario 1 illustrates the case of *limited radio and computing resources* and is characterized by parameters $B_t = 15\,\text{MB}$ [16], $R_0^t = 100\,\text{Mbps}$ [16], $B_c = 30\,\text{MB}$ [17], $R_0^c = 20\,\text{GHz}$, [19]. Scenario 2 corresponds to *limited computing* resources and *abundant radio* resources as given by $R_0^t = 3000\,\text{Mbps}$. Further, we focus on the case of *abundant radio and computing resources* that is illustrated by $R_0^t = 3000\,\text{Mbps}$, $R_0^c = 175\,\text{GHz}$ [20], which is Scenario 3. Table II summarizes the main system parameters.

In Fig. 2, we assess the performance of our XR system under Scenario 1. The numbers of active users involved in the communication and processing phases increase with a cyclic trend governed by our periodic arrival rate function. The uplink transmission rate and processing speed decrease, which triggers the rising delays. Here, the availability of 100 Mbps of the total uplink capacity and 20 GHz of the total edge node processing capacity is insufficient for the uplink packet size of 15 MB and downloaded content size of 30 MB.

For Scenario 1, the bottleneck manifests during both the communication and the processing phases. Conventional system configurations may fail to support seamless low-latency XR experience, thereby calling for improved network capacities. System designers may thus consider distributed computing to reduce the computation times for video processing at the edge server. In addition, beyond-5G cellular networks with multi-RAT, multi-connectivity functionalities, and content-aware edge-node deployments may become promising for the emerging XR-ready systems.

In Fig. 3, we consider Scenario 2. Our results demonstrate that the availability of 3000 Mbps of the total uplink capacity ensures low-latency uplink transmissions. However, the processing procedure for the XR video remains demanding. At time instant $t = 221\,\text{s}$, no further content requests

[1]Measured as R_0^t / N_k^{at}.
[2]Measured as $R_0^c / (N_k^{ac}(N_k^{ac} + \alpha))$.

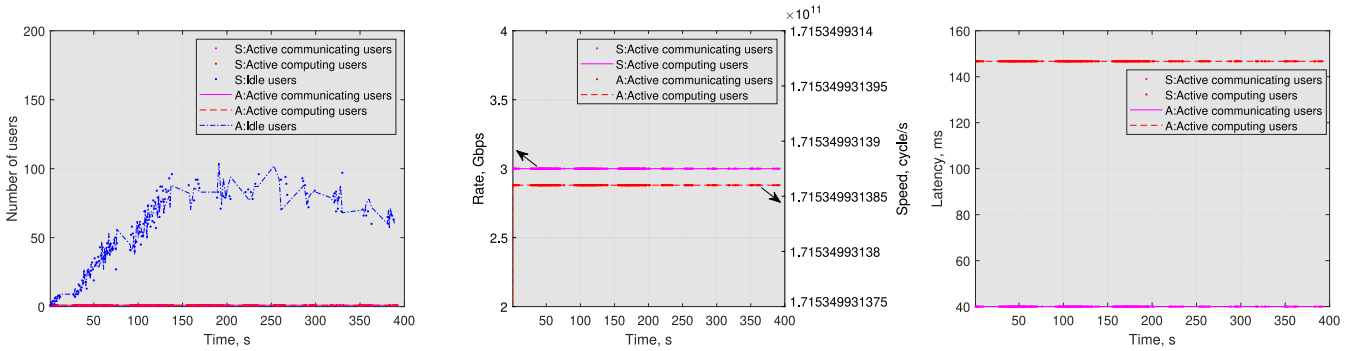

(a) Number of users (b) Actual transmission rate/processing speed (c) Latency

Fig. 4. Performance assessment (Scenario 3): $B_t = 15\,\text{MB}$, $R_0^t = 3000\,\text{Mbps}$, $B_c = 30\,\text{MB}$, $R_0^c = 175\,\text{GHz}$.

arrive in the system, thus leading to its gradual unloading, a decrease in the number of computing users, and, hence, a decline in latency. As per our additional results, a scenario with limited communication and abundant computation resources yields qualitatively similar observations but with an opposite trend between the communication and the computing resources.

Further, as shown in Fig. 4, our findings demonstrate that the availability of 3000 Mbps of the total uplink capacity and 175 GHz of the edge node processing capacity can support low-latency communications assuming typical uplink packet size, B_t, of 15 MB and content size, B_c, of 30 MB. Based on the reported evaluation, we may conclude that today's 5G NR deployments may encounter challenges in supporting the required latency for seamless XR user experience in the case of large social/public events.

V. Conclusion

In this letter, we presented our methodology to characterize user and content dynamics of immersive reality services in wireless networks with non-stationary arrival processes, i.e., a periodic arrival rate function. This approach considered both communication and computing resources to capture the time and space dynamics of users engaged in XR content exchange. We validated our analytical method to assess the system operation under various network configurations. The uplink transmission for XR is highly demanding in terms of radio resources, as it requires a minimum of 3000 Mbps for the packet size of 15 MB. The computation procedure for XR video processing appears to also be demanding in terms of computational resources by requiring more than 175 GHz to process the model of 30 MB. To provide effective support for XR experience, future research may explore artificial intelligence-based resource optimization as well as consider mobility patterns specific to XR applications.

References

[1] Oculus. "Introducing Oculus air link, a wireless way to play PC VR games on Oculus Quest 2, plus infinite office updates, support for 120 Hz on Quest 2, and more." 2021. [Online]. Available: https://www.oculus.com/blog/

[2] A. Ali, O. Galinina, and S. Andreev, "System-level dynamics of highly directional distributed networks," *IEEE Wireless Commun. Lett.*, vol. 10, no. 7, pp. 1523–1527, Jul. 2021.

[3] M. Lecci, F. Chiariotti, M. Drago, A. Zanella, and M. Zorzi, "Temporal characterization of XR traffic with application to predictive network slicing," 2022, *arXiv:2201.07043*.

[4] A. U. Rahman, G. Ghatak, and A. De Domenico, "An online algorithm for computation offloading in non-stationary environments," *IEEE Commun. Lett.*, vol. 24, no. 10, pp. 2167–2171, Oct. 2020.

[5] F. Alriksson et al., "XR and 5G: Extended reality at scale with time-critical communication," *Ericsson Technol. Rev.*, vol. 2021, no. 8, pp. 2–13, 2021.

[6] K. K. Leung, W. A. Massey, and W. Whitt, "Traffic models for wireless communication networks," *IEEE J. Sel. Areas Commun.*, vol. 12, no. 8, pp. 1353–1364, Oct. 1994.

[7] D. Qiu and R. Srikant, "Modeling and performance analysis of BitTorrent-like peer-to-peer networks," *ACM SIGCOMM Comput. Commun. Rev.*, vol. 34, no. 4, pp. 367–378, 2004.

[8] A. Pyattaev, O. Galinina, S. Andreev, M. Katz, and Y. Koucheryavy, "Understanding practical limitations of network coding for assisted proximate communication," *IEEE J. Sel. Areas Commun.*, vol. 33, no. 2, pp. 156–170, Feb. 2015.

[9] C. Sergiou and V. Vassiliou, "Estimating maximum traffic volume in wireless sensor networks using fluid dynamics principles," *IEEE Commun. Lett.*, vol. 17, no. 2, pp. 257–260, Feb. 2013.

[10] M. Armbrust et al., *Above the Clouds: A Berkeley View of Cloud Computing*, Univ. California at Berkeley, Berkeley, CA, USA, 2016.

[11] D. Bruneo, "A stochastic model to investigate data center performance and QoS in IaaS cloud computing systems," *IEEE Trans. Parallel Distrib. Syst.*, vol. 25, no. 3, pp. 560–569, Mar. 2014.

[12] A. I. Sulyman, A. T. Nassar, M. K. Samimi, G. R. MacCartney, T. S. Rappaport, and A. Alsanie, "Radio propagation path loss models for 5G cellular networks in the 28 GHz and 38 GHz millimeter-wave bands," *IEEE Commun. Mag.*, vol. 52, no. 9, pp. 78–86, Sep. 2014.

[13] H. Wymeersch and G. Seco-Granados, "Radio localization and sensing—Part II: State-of-the-art and challenges," *IEEE Commun. Lett.*, vol. 26, no. 12, pp. 2821–2825, Dec. 2022.

[14] Y. He, D. Wang, F. Huang, and R. Zhang, "An MEC-enabled framework for task offloading and power allocation in NOMA enhanced ABS-assisted VANETs," *IEEE Commun. Lett.*, vol. 26, no. 6, pp. 1353–1357, Jun. 2022.

[15] A. Forde and J. Daniel, "Pedestrian walking speed at un-signalized mid-block crosswalk and its impact on urban street segment performance," *J. Traffic Transp. Eng.*, vol. 8, no. 1, pp. 57–69, 2021.

[16] "3rd generation partnership project; technical specification group services and system aspects; extended reality (XR) in 5G (Release 17), v17.0.0," 3GPP, Sophia Antipolis, France, Rep. TR 26.928, Apr. 2022.

[17] F. Hu, Y. Deng, H. Zhou, T. H. Jung, C.-B. Chae, and A. H. Aghvami, "A vision of an XR-aided teleoperation system toward 5G/B5G," *IEEE Commun. Mag.*, vol. 59, no. 1, pp. 34–40, Jan. 2021.

[18] J. Liang, H. Xing, F. Wang, and V. K. Lau, "Joint task offloading and cache placement for energy-efficient mobile edge computing systems," *IEEE Wireless Commun. Lett.*, vol. 12, no. 4, pp. 694–698, Apr. 2023.

[19] X. Lyu, H. Tian, C. Sengul, and P. Zhang, "Multiuser joint task offloading and resource optimization in proximate clouds," *IEEE Trans. Veh. Technol.*, vol. 66, no. 4, pp. 3435–3447, Apr. 2017.

[20] S. Gupta, J. Chakareski, and P. Popovski, "mmWave networking and edge computing for scalable 360 ° video multi-user virtual reality," *IEEE Trans. Image Process.*, vol. 32, pp. 377–391, 2022.